Fibrosis Effects on Strain and Volumetric Metrics in Left Atrial Simulations

Åshild Telle[1,2], Ahmad Kassar[3], Romanos Haykal[3], Kaviya Muralidharan[1],
Juan Carlos del Álamo[1,3], Nazem Akoum[3], Christoph M. Augustin[4], Patrick M. Boyle[1,2,3]

[1] Department of Bioengineering, University of Washington, Seattle, WA, USA
[2] eScience Institute, University of Washington, Seattle, WA, USA
[3] Division of Cardiology, Department of Medicine, University of Washington, Seattle, WA, USA
[4]Gottfried Schatz Research Center, Division of Medical Physics and Biophysics,
Medical University of Graz, Graz, Austria

Abstract

Left atrial (LA) strain is clinically used to assess LA function, yet its relationship to underlying mechanics and fibrosis remains incompletely understood. We here used a physiologically detailed 3D LA electromechanical–0D circulatory model to evaluate fibrosis-induced changes, combined with patient-specific geometries from atrial fibrillation (AF) and embolic stroke of undetermined source (ESUS) cohorts. Reservoir (total), booster (active), and conduit (passive) function were quantified using volumetric indices (emptying fraction, EF), 3D fiber-direction strain, and 2D cross-sectional strain. Booster function showed the largest fibrotic reductions, with highest relative differences in 2D strain (47% reduction from baseline) and strongest correlation with fibrosis burden in 3D strain ($R^2 = 0.84$). Our findings show that computational models reproduce fibrotic effects within clinically representative ranges and may help bridge computational modeling with clinical assessment.

1. Introduction

Volumetric and strain-based LA function metrics are important clinical biomarkers of cardiac performance and cardiovascular disease. Volumetric indices quantify blood-flow performance, while strain metrics capture myocardial deformation and may reveal early dysfunction [1]. LA function is commonly divided into reservoir, booster, and conduit components, reflecting on atrial contraction and ventricular filling. Fibrotic remodeling reduces contractility and increases tissue stiffness, lowering these metrics [2]. Common among AF and ESUS patients, LA fibrosis contributes to increased ischemic stroke risk [3].

Clinical evaluation relies primarily on imaging. Strain is commonly measured over a 2D cross-section of the LA body, capturing longitudinal deformation throughout the cardiac cycle. 3D approaches are emerging, but require more advanced acquisition and post-processing procedures [4, 5]. Volumetric measurements can be obtained in both 2D (estimated) and 3D. High-fidelity computational models can reproduce all these metrics, yet model-predicted 2D strain remains unreported.

In this study, we introduce a computational analog of clinical 2D cross-sectional strain. We compare it with 3D fiber-direction strain and volumetric metrics, focusing on sensitivity to fibrotic remodeling. These relationships can support model validation and personalization.

2. Methods

2.1. Patient recruitment

We obtained patient-specific LA geometries and corresponding fibrotic distributions from AF and ESUS cohorts (Table 1). Participants were recruited at the University of Washington Medical Center, and the study was approved by the University of Washington Institutional Review Board (STUDY00015081). Written informed consent was obtained from all patients. Fibrosis distributions were derived from MRI with late gadolinium enhancement (MRI LGE) (Table 1, Fig. 1). Total EF and reservoir, booster, and conduit strain from cardiac MRI 2D cross-sections were collected for calibration.

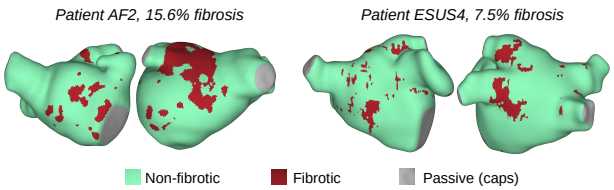

Figure 1. Patient geometries AF2 and ESUS4 with corresponding MRI LGE-derived fibrotic distributions.

Table 1. Patient-specific demographics and clinical measurements

Patient	Age	Sex	LA EDV (mL)	LV EDV (mL)	LAF (%)
AF1	66	M	82.2	125.2	18.9
AF2	81	F	145.1	126.3	15.6
AF3	70	M	121.6	179.8	22.0
AF4	63	M	141.5	124.0	23.9
ESUS1	56	M	66.5	143.3	6.5
ESUS2	81	F	105.9	147.9	14.0
ESUS3	71	F	78.3	79.9	16.5
ESUS4	76	M	90.8	125.7	7.5
ESUS5	45	F	31.5	156.5	37.6

LA/LV EDV = LA/LV end-diastolic volume; LAF = LA fibrosis burden

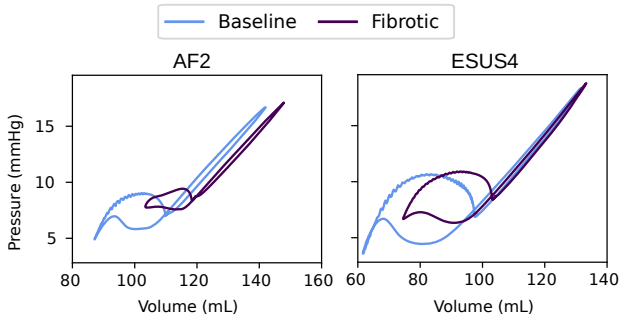

Figure 2. Pressure-volume loops for patients AF2 and ESUS4, baseline (predicted) versus fibrotic (calibrated) simulations.

2.2. Computational modeling framework

LA function was simulated using a 3D electromechanical–0D circulatory model [6, 7]. Simulations were performed using Carpentry (NumeriCor GmbH), an extension of openCARP (www.opencarp.org). Pericardial stiffness was represented by a spatially varying normal-spring boundary condition, highest at the LA roof and lowest near the mitral valve [8]. LA active tension, ventricular sarcomere dynamics, atrioventricular traction, and systemic flow parameters were tuned to match patient ranges (fibrotic simulations). Patient-specific LV end-diastolic volumes (Table 1) were prescribed in the circulatory model.

In fibrotic simulations, nine electromechanical parameters (prescribing reduced conduction velocities and ionic currents, reduced contractility, and increased stiffness) were modified within fibrotic regions [7]. Systemic resistance factor was set to 0.75 at baseline and 1.25 in fibrotic simulations, representing differences in blood pressure. Model-predicted pressure–volume loops for two patients are shown in Fig. 2.

2.3. LA function assessment

LA function was quantified using three complementary modalities: EF, 3D fiber-direction strain, and 2D cross-sectional strain (Fig. 3). EF metrics were calculated from maximum, pre-contraction, and minimum volumes. 3D fiber-direction strain was computed in ParaView by tracking Green-Lagrange fiber-direction strain with the *Plot Over Time* filter. 2D cross-sectional strain was obtained from a fixed plane defined by the middle anterior and posterior mitral annulus points and the LA roof at maximum LA volume. The plane–mesh intersection was next processed using *Feature Edges*, *Integrate Variables*, and *Plot Over Time* (Field Association: Cells) filters to track boundary-length changes over time.

Each modality had reservoir, conduit, and booster components. Simulations were initiated with LA contraction and were therefore inherently P–P gated. Time series were normalized and mapped to R–R gating using mitral valve closure (LA systole) as reference. Reservoir strain was defined as maximum value, while conduit and booster strain were evaluated at initial LA activation.

Statistical differences between baseline and fibrotic outputs were assessed with two-sample t-tests. Correlations with fibrosis burden were quantified by linear regression.

3. Results

Time transients and derived metrics for all simulations are shown in Fig. 4. Booster function was most impaired comparing fibrotic to baseline (mean decrease 35% for EF, 40% for 3D strain, and 47% for 2D strain). Reservoir function showed moderate impairment (with 22%, 33%, and 33%, respectively), and conduit function least (13%, 11%, and 10%). Active and reservoir metrics, together with passive EF and conduit 3D strain, were significantly reduced ($p < 0.05$), whereas conduit 2D strain was not.

Compared to clinical data (Fig. 4B), our fibrotic simulations underestimated total EF (14.0±8.1% on average). Strain measurements were reasonably captured, with mean deviations of 0.6±4.2% for reservoir, 0.14±3.5% for booster, and 3.1±3.2% for conduit strain.

Scatter plots and linear regression fits for fibrotic simulations are shown in Fig. 5. Booster 3D fiber-direction strain (middle panel) exhibited the strongest correlation with fibrotic burden ($R^2 = 0.84$). Passive function exhibited weak correlation across all modalities.

4. Discussion

This study compared strain- and volume-based LA metrics derived from computational simulations. It demonstrates the feasibility of matching clinically relevant measures for model validation and parameterization.

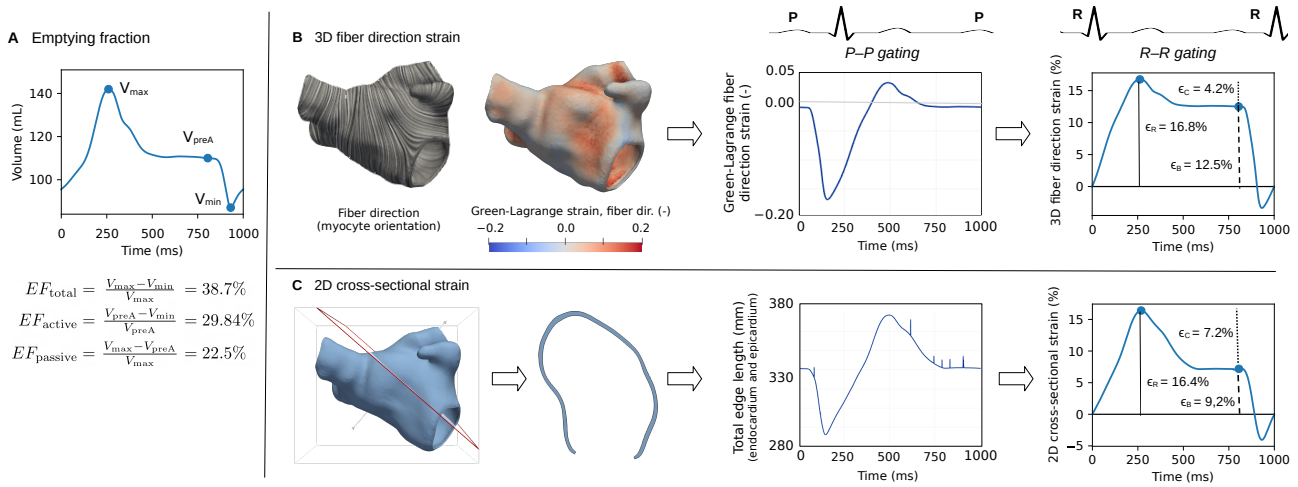

Figure 3. Overview of LA function metrics: (A) Volume over time, with volumetric measurements (V_{max}, V_{preA}, V_{min}) marked, and EF metric definitions. (B) 3D fiber-direction strain, derived from by Green–Lagrange fiber direction strain over time. (C) Cross-sectional 2D strain, obtained from boundary-length changes over time. Strain curves were normalized and mapped to R–R gating, from which we obtained reservoir (ϵ_R), booster (ϵ_B), and conduit (ϵ_C) components.

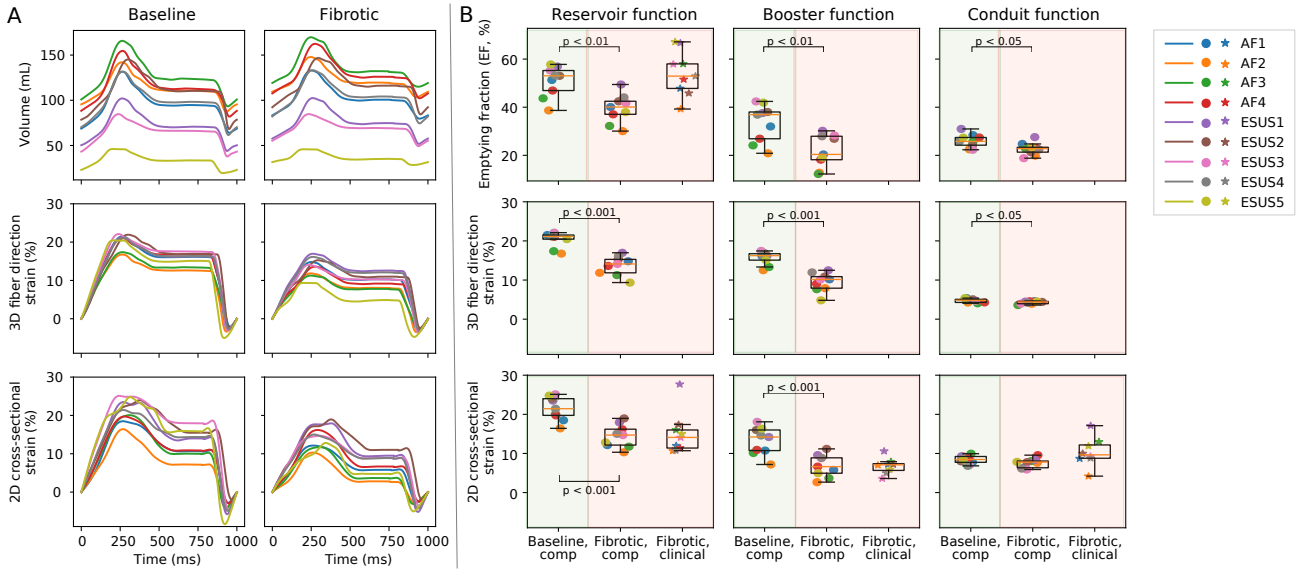

Figure 4. Baseline versus fibrotic effect on volumetric and strain-based metrics. (A) Time transients for baseline versus fibrotic simulations. (B) Computationally predicted total, active, and passive function measurements (dots), baseline versus fibrotic, alongside clinical measurements (stars) of total EF and (2D) reservoir, booster, and conduit strain.

Model-predicted 2D strain showed largest magnitude differences under fibrotic remodeling, whereas 3D strain correlated more strongly with fibrosis burden. This aligns with findings by Sillett et al. [5] and Mochizuki et al. [9], who reported 3D fiber-direction strain to best correlate with AF occurrence. Beyond capturing global deformation, 3D fiber strain likely better reflects fibrotic effects by capturing tensile changes along fibers rather than chamber-wise radial deformation.

Booster function was more impaired than conduit and reservoir function in our simulations. This contrasts with clinical studies [10–12], where reservoir function is most consistently impaired. In our work, fibrosis-related parameter changes primarily affected LA contraction, while conduit function was influenced mainly by stiffness and systemic flow. This suggests that our parameterization reasonably captures fibrotic reductions in booster function, whereas conduit mechanisms require further studies.

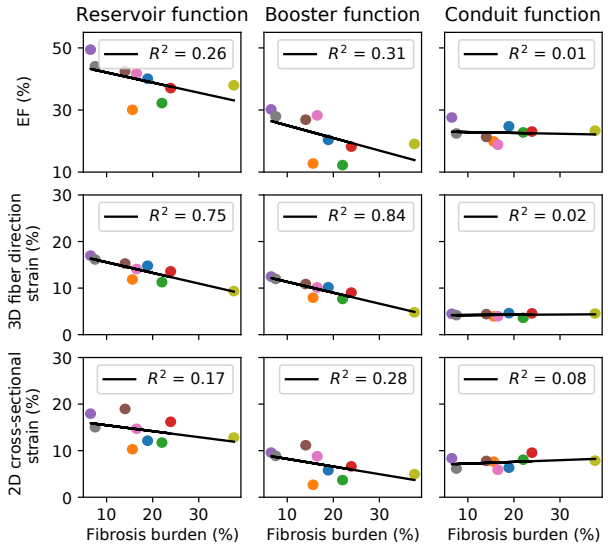

Figure 5. Correlation between LA function metrics and fibrosis burden for fibrotic simulations. Individual patients (dots) color-coded as in Fig. 4.

An important limitation is that our model did not reproduce patient-specific passive or total EF ranges. Similarly baseline (healthy) values were below reference ranges [7, 13]. We also used generic fiber orientation and wall-thickness fields, applied homogeneous parameter changes within fibrotic regions and none in non-fibrotic regions, all simplified representations of complex human physiology.

Future work may support robust patient-specific digital-twin development and quantitatively separate fibrotic from volumetric remodeling. Coupling these models with fluid dynamics could clarify thrombogenesis mechanisms in AF- or ESUS-related atrial myopathies.

References

[1] Thomas L, Marwick TH, Popescu BA, Donal E, Badano LP. Left atrial structure and function, and left ventricular diastolic dysfunction: JACC state-of-the-art review. J Am Coll Cardiol 2019;73(15):1961–1977.

[2] Kuppahally SS, Akoum N, Burgon NS, Badger TJ, Kholmovski EG, Vijayakumar S, Rao SN, Blauer J, Fish EN, Dibella EV, et al. Left atrial strain and strain rate in patients with paroxysmal and persistent atrial fibrillation: relationship to left atrial structural remodeling detected by delayed-enhancement MRI. Circ Cardiovasc Imaging 2010; 3(3):231–239.

[3] Mahnkopf C, Kwon Y, Akoum N. Atrial fibrosis, ischaemic stroke and atrial fibrillation. AER 2021;10(4):225.

[4] Yafasov M, Olsen FJ, Hauser R, Skaarup KG, Lassen MCH, Johansen ND, Lindgren FL, Søgaard P, Jensen GB, Schnohr P, et al. Left atrial strain measured by three-dimensional echocardiography predicts atrial fibrillation in the general population. Int J Cardiol 2024;417:132544.

[5] Sillett C, Razeghi O, Lee AW, Solis Lemus JA, Roney C, Mannina C, De Vere F, Ananthan K, Ennis DB, Haberland U, et al. A three-dimensional left atrial motion estimation from retrospective gated computed tomography: application in heart failure patients with atrial fibrillation. Front Cardiovasc Med 2024;11:1359715.

[6] Augustin CM, Gsell MA, Karabelas E, Willemen E, Prinzen FW, Lumens J, Vigmond EJ, Plank G. A computationally efficient physiologically comprehensive 3D–0D closed-loop model of the heart and circulation. Comput Methods Appl Mech Eng 2021;386:114092.

[7] Telle Å, Kassar A, Chamoun N, Haykal R, Gonzalo A, Hensley T, Chahine Y, Flores O, Del Álamo JC, Akoum N, et al. Systematic computational assessment of atrial function impairment due to fibrotic remodeling in electromechanical properties. PLOS Comput Biol 2025; 21(12):e1013265.

[8] Baptiste TM, Rodero C, Sillett CP, Strocchi M, Lanyon CW, Augustin CM, Lee AW, Solís-Lemus JA, Roney CH, Ennis DB, et al. Regional heterogeneity in left atrial stiffness impacts passive deformation in a cohort of patient-specific models. PLOS Comput Biol 2025;21(11):e1013656.

[9] Mochizuki A, Yuda S, Fujito T, Kawamukai M, Muranaka A, Nagahara D, Shimoshige S, Hashimoto A, Miura T. Left atrial strain assessed by three-dimensional speckle tracking echocardiography predicts atrial fibrillation recurrence after catheter ablation in patients with paroxysmal atrial fibrillation. J Echocardiogr 2017;15(2):79–87.

[10] Inoue YY, Alissa A, Khurram IM, Fukumoto K, Habibi M, Venkatesh BA, Zimmerman SL, Nazarian S, Berger RD, Calkins H, et al. Quantitative tissue-tracking cardiac magnetic resonance (CMR) of left atrial deformation and the risk of stroke in patients with atrial fibrillation. J Am Heart Assoc 2015;4(4):e001844.

[11] Hopman LH, Mulder MJ, van der Laan AM, Demirkiran A, Bhagirath P, van Rossum AC, Allaart CP, Götte MJ. Impaired left atrial reservoir and conduit strain in patients with atrial fibrillation and extensive left atrial fibrosis. J Cardiovasc Magn Reson 2021;23(1):131.

[12] Olsen FJ, Bertelsen L, Vejlstrup N, Diederichsen SZ, Bjerregaard CL, Graff C, Brandes A, Krieger D, Haugan K, Køber L, et al. Association between four-dimensional echocardiographic left atrial measures and left atrial fibrosis assessed by left atrial late gadolinium enhancement. Eur Heart J Cardiovasc Imaging 2023;24(1):152–161.

[13] Singh A, Singulane CC, Miyoshi T, Prado AD, Addetia K, Bellino M, Daimon M, Fajardo PG, Kasliwal RR, Kirkpatrick JN, et al. Normal values of left atrial size and function and the impact of age: results of the world alliance societies of echocardiography study. J Am Soc Echocardiogr 2022;35(2):154–164.

Address for correspondence:

Å Telle (aashild@uw.edu) or PM Boyle (pmjboyle@uw.edu)
3720 15th Ave NE, Seattle, WA 98195, USA